第 20 卷第 9 期　　半 导 体 学 报　　Vol. 20, No. 9
1999 年 9 月　　CHINESE JOURNAL OF SEMICONDUCTORS　　Sep., 1999

Effects of Sputtering Power on Structural, Electrical and Optical Properties of Indium-tin-oxide Thin Films*

Wang Zhongchun (王忠春), Chen Jiefeng (陈杰锋), Hu Xingfang (胡行方)

(Shanghai Institute of Ceramics, The Chinese Academy of Sciences, Shanghai 200050)

Abstract Indium tin oxide (ITO) thin films were deposited on a RF diode sputtering system under different sputtering voltages and optimized sputtering ambient, i.e. optimized O_2 partial pressure and total pressure of O_2 and Ar. The morphology, structure and oxygen deficiency of the ITO films were studied using atomic force microscopy (AFM), X-ray diffractogram (XRD) and X-ray photoelectron spectroscopy (XPS), respectively. As indicated by the results, the films deposited under higher sputtering voltage showed higher crystal order and larger oxygen deficiency. The optimization work has led to the production of ITO films with a resistivity as low as $1.76\times10^{-4}\Omega\cdot$cm, an integrated luminous transmittance of 76.0% and an integrated solar transmittance of 52.5% with no substrate heating or post-deposition annealing.

PACC: 8115G, 7360F, 7865

1 Introduction

Indium tin oxide, commonly referred to as ITO, is a wide band gap, degenerate n-type semiconductor. In the form of thin film, it has wide applications in optics and optoelectronics[1], such as flat panel displays[2,3], heat mirrors[4], and heterojunction solar cells[5], etc. High electrical conductivity and high transparency of this material in the visible spectrum range have been the focus of research throughout the world.

A variety of techniques have been used to deposit ITO thin films, such as sputtering[5,6], electron beam evaporation[7], CVD[8] and spray pyrolysis[9], etc. Among them, sputtering technology is favored owing to the possibility of largely improving its deposition rate up to industrial level[10]. Deposition parameters influencing the electrical and optical prop-

* Project supported by the National Climbing Program of China (Grant No. 07-01) and the National Natural Science Foundation of China (Grant No. 59782006).

Dr. Wang Zhongchun (王忠春), born in 1967, is now a research assistant, whose research interest lies in the synthesis and opto-electronics of novel thin film materials.

Prof. Chen Jiefeng (陈杰锋) was born in 1944, who are interested in the thermo-optical properties of thermal control coatings for spacecraft.

Prof. Hu Xingfang (胡行方) was born in 1936, who has great interest in electrochromic materials for Smart Windows.

Received 17 December 1998, revised manuscript received 15 May 1999

erties of ITO thin films have been extensively studied[1], which include In/Sn ratio, incident angle, substrate temperature, deposition rate, total pressure, O_2 partial pressure and annealing conditions, etc. However, few studies on the effects of sputtering power have been reported[11].

Modern applications employing ITO thin films use often substrates with low thermal stability[12]. For example, when acting as the antireflecting layers of solar cells or the transparent conducting layers of electrochromic windows, ITO thin films should not be deposited under temperatures so high that the performances of the whole devices will be lowered or even disappear. The application background of this work is acting as the transparent conducting layers of electrochromic windows, and so we chose to deposit the ITO thin films with no substrate heating or post-deposition annealing. In this paper, two kinds of samples, representative of two typical sputtering power densities respectively, were investigated and the results were discussed.

2 Experimental

ITO thin films were prepared by using a 450-D RF diode sputtering system. Reactive sputtering took place from a sintered target (90wt. % In_2O_3-10wt. % SnO_2 and 10cm in diameter) in an optimized plasma containing Ar (99.99%) and O_2 (99.99%) under different sputtering powers. The sputtering power was adjusted by applied voltages, and two samples, denoted below as # 1 and # 2 respectively, were deposited under two typical voltages. The atmosphere pressure was maintained by gas inlet via a needle valve. The distance between the target and the substrate was 9cm. The substrates were placed on a water-cooled platform. Before deposition, the target was presputtered for 25min. Microscope slides were used as substrates for electrical and optical measurements, while polished silicon single crystal (100) was used for atomic force microscopy (AFM) analysis.

Film thickness was determined by a Talystep profilemeter (Rank Taylor Hobson). Sheet resistance of samples was measured with a four-point probe. The surface morphology of the films was recorded by AFM using a NanoScope Ⅲ instrument in contact mode. The structure of the films was checked out by X-ray diffraction (Nippon Rigaku RAX ra-10). Optical transmittance and reflectance spectra were measured using a CARY 2390 spectrophotometer with an integrating sphere. XPS spectra were recorded on a MICRO LAB MK Ⅱ surface analyzer with a Mg anode, and all spectra were calibrated with the Au $4f_{7/2}$ peak at 83.8eV.

Deposition parameters and some properties of ITO thin films # 1 and # 2 are detailed in Table 1.

Table 1 Deposition parameters and properties of ITO thin films

Sample	# 1	# 2
Sputtering voltage/V	2600	1600
O_2 partial pressure/×0.13332Pa	3	3
Total pressure/×133.32Pa	0.1	0.1
Thickness/nm	440	400
Deposition rate/ (nm·min^{-1})	17.6	20.0
Resistivity/ (×10^{-4}Ω·cm)	1.76	11.4
RMS roughness/nm	6.569	0.998
Maximum peak-valley distance/nm	50.634	8.034
Binding energy for In $3d_{3/2}$/eV	452.2	452.0
Binding energy for In $3d_{5/2}$/eV	444.6	444.4

3 Results and discussion

3.1 Electrical and optical properties

Resistivity ρ of thin films can be calculated according to

$$\rho = R_{sh} d$$

where R_{sh} is the sheet resistance; d is the thickness of the film. Results are listed in Table 1. It is seen that ρ of ITO # 2 is nearly one order of magnitude higher than that of # 1.

The lowest value of resistivity for ITO films reported in the literature[13] is about 2×10^{-4}Ω·cm, but substrate heating was used during deposition. The resistivity of ITO # 1 is as low as 1.76×10^{-4}Ω·cm. So it is possible to reduce the resistivity of ITO films to 2×10^{-4}Ω·cm or even lower under proper sputtering atmosphere, especially proper oxygen partial pressure, with no substrate heating or post-deposition annealing, meanwhile keeping sufficiently high visible transmittance.

Spectral characteristics of ITO films in the visible and solar spectrum range are shown

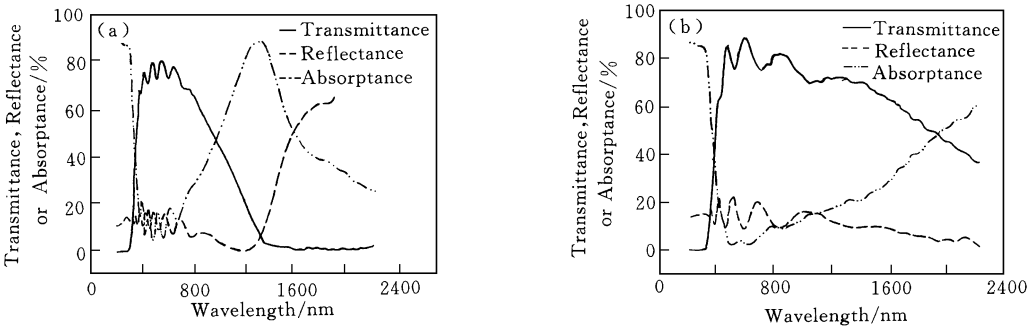

FIG. 1 Visible and solar spectral properties of ITO thin films
(a) ITO # 1; (b) ITO # 2

in Fig. 1. Visible integrated transmittances T_{vis} of ITO # 1 and # 2 were calculated to be 76.0% and 82.1% respectively, while solar integrated transmittances T_{sol} 52.5% and

70.2% respectively. For both T_{vis} and T_{sol}, ITO # 2 is higher than # 1, but their spectral characteristics differ a lot. As seen in Fig. 1, ITO # 1 has a plasma absorption peak around 1320nm, while for ITO # 2, such a peak does not appear, at least within the measured spectrum range. According to the Drude theory, wavelengths for plasma resonance absorption decrease with increasing free carrier density, and vice versa. The above results show that electron density of ITO # 1 is much higher than that of # 2. Fortunately, high reflection of ITO # 1 occurs in the NIR region, and there is little effect on its visible transmittance, however its solar transmittance has been reduced considerably.

3.2　Structural features observed by AFM

Fig. 2 shows the AFM images of ITO # 1 and # 2. Judged by their rms roughness and maximum peak-valley distances, as shown in Table 1, ITO # 2 is far smoother than # 1. In face, if the scan area for ITO # 2 in Fig. 2 (b) was reduced to $1\mu m^2$, clear images could not be obtained due to the limited resolution capacity of the instrument. But it can be seen from Fig. 2 that # 1 is much denser than # 2, which can partly explain the controversial deposition rates reported in Table 1. From Fig. 2, average crystallite sizes were estimated to be 50 and 40nm for ITO # 1 and # 2 respectively.

For ITO # 1, which was deposited under higher sputtering power, the particles sputtered out from the target has higher kinetic energy, and higher-energy particles bombarding the substrates can lead to temperature ascending, both of which are beneficial to crystal growth. In Fig. 2 (a), one can clearly see that the columnar crystallites, numbered around 5～8, grow in between the grain boundaries to form larger clusters, resulting in shrinkage or even disappearance of grain boundaries. As grain boundaries scatter electrons, this will largely improve the electron mobility, and hence reduce the electrical resistivity of ITO # 1.

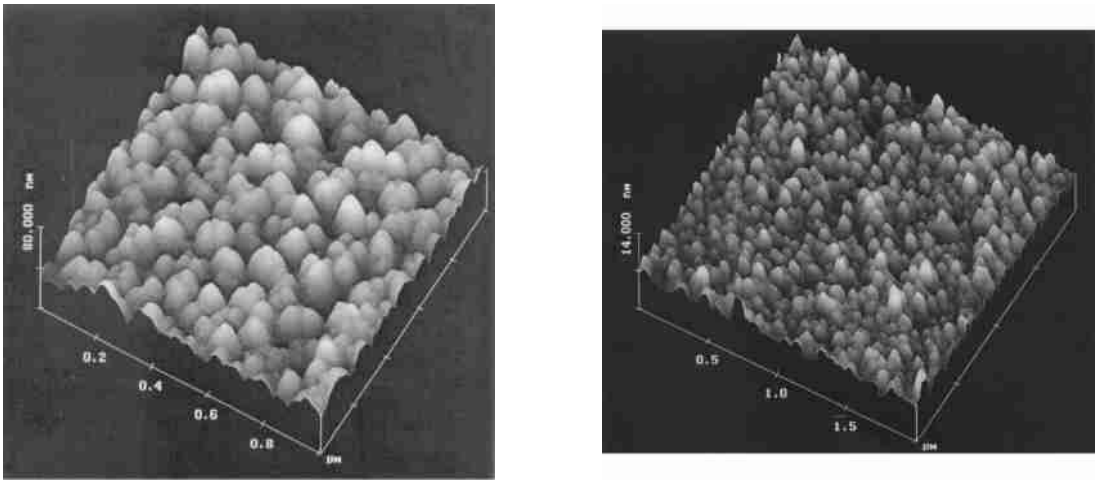

(a)　　(b)

FIG. 2　AFM images of ITO thin films deposited on Si substrates
(a) ITO # 1; (b) ITO # 2

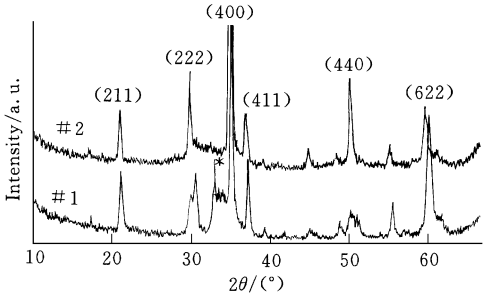

FIG. 3 XRD patterns of ITO thin films # 1 and # 2, deposited on glass substrates

3.3 XRD analysis

Nearly all the diffraction peaks in Fig. 3 can be indexed by assuming the C-type rare-earth oxide structure (JCPDS card # 6-0416). The intensity of the highest peak (400) for # 1 is much higher than that for # 2, which indicates that # 1 has higher degree of crystal order compared to # 2, in consistency with the above AFM observations.

For ITO # 1, weak broad peaks accompany with the three peaks for (222), (400) and (622), indicating the existence of impure or non-crystalline phases. As an example, the peak around the diffraction angle of 33°, marked with '*', can be attributed to the (320) reflection for the compound $In_2Sn_2O_{7-x}$ (JCPDS # 39-1058).

Contrary to the standard In_2O_3 powder pattern in which the strongest peak is (222), both films # 1 and # 2 show (400) preferred orientation. It is reported that the crystallization of ITO along (400) plane requires less energy than that required for the crystallization along (222) plane[14]. Concisely, (222) is thermodynamically preferred while (400) is kinetically preferred. We deposited the films at near room temperature, which is expected to reduce the thermal mobility of the adatoms on the substrates, and hence the films are preferentially oriented in < 100> direction.

3.4 XPS analysis

Binding energies for In $3d_{3/2}$ and In $3d_{5/2}$ in ITO # 1 and # 2 are listed in Table 1, and are found to be in well agreement with literature values[15]. No appreciable difference in the chemical states of In is observed between ITO films prepared under different sputtering powers. The conductivity of ITO is n-type as a result of oxygen vacancies and the presence of tin dopant which has a higher valence than indium. The extra electronic charge in the ITO films is trapped only at oxygen vacancies and Sn centers, and the In $3d_{3/2}$ or In $3d_{5/2}$ peaks should be insensitive to the loss of oxygen and to the Sn concentration.

However, O 1s XPS spectra of ITO # 1 and # 2, shown in Fig. 4 (a) and 4 (b) respectively, exhibit differences. Using two Gaussian functions with variable positions, widths and intensities, the O 1s peaks were fitted, after deduction of the background, by two peaks located around 532eV and 530eV, referred to as O_{I} and O_{II} respectively.

In_2O_3 exhibits the cubic bixbyite structure. It shows a fluorite-related superstructure where one-fourth of the anions are missing. Each cationic site can be described as a cube where two anion sites are empty at opposite vertices for *b* sites and along one diagonal of a face for *d* sites[16]. As a consequence, the oxygen anions can be classified into two categories: near and away from the structural oxygen vacancies (referred to as O_{I} and O_{II}, re-

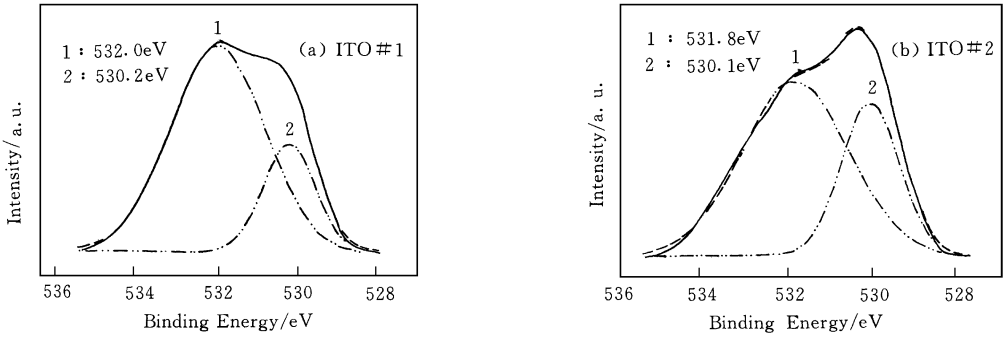

FIG. 4 O 1s XPS spectra of ITO thin films
(a) ITO# 1; (b) ITO# 2

spectively). The ratio of O_I/O_{II} is 2∶1. In comparison with those in O_{II}, the outer-layer electrons in O_I are more strongly attracted by the surrounding cations, and have less screening effect to the inner-layer electrons. So the binding energies of O 1s for O_I should be higher than for O_{II}. Therefore, the intensity of O_I peak will increase with increasing oxygen deficiency, and the area ratio of O_I/O_{II} can be taken as an indicator of oxygen deficiency.

As calculated from Fig. 4, the area ratio of O_I/O_{II} is 2.1∶1 for ITO# 2, while 3.5∶1 for ITO# 1. Clearly, oxygen deficiency in ITO# 1 is higher than that in ITO# 2. At higher sputtering power, the particle ejection rate from the target is faster, and more oxygen is needed to compensate for its consumption. At the same level of oxygen partial pressure and total pressure, the result will naturally be that ITO# 1 has higher oxygen deficiency, and hence higher carrier density that # 2.

4 Conclusion

In this work, ITO thin films have been deposited by RF diode reactively sputtering technique under different sputtering powers at near room temperature. It is demonstrated that the ITO film, deposited at optimum oxygen partial pressure and higher sputtering power, has higher crystal order and oxygen deficiency, which results in its low electrical resistivity of $1.76\times10^{-4}\Omega\cdot$cm, meanwhile keeping its visible integrated transmittance up to 76.0%. The results indicate that it should be possible to produce large area ITO for electrochromic windows with sufficiently low sheet resistance coupled with high visible transmittance.

Acknowledgement: Dr. Chen Jie from University of Science and Technology of China is gratefully acknowledged for his great help in this work.

References

[1] H. L. Hartnagel, A. L. Dawar, A. K. Jain and C. Jagadish, Semiconducting Transparent Thin Films, Institute of Physics Publishing, Bristol and Philadelphia, 1995.

[2] J. E. Costellamo, Handbook of Display Technology, Academic Press, New York, 1992.

[3] S. Ishibashi, Y. Higuchi, Y. Ota and K. Nakamura, J. Vac. Sci. Technol., 1990, **A8**: 1399.

[4] K. L. Chopra and S. R. Das, Thin Film Solar Cells, Plenum Press, New York, 1983, p321.

[5] C. V. R. Vasant Kumar and A. Man Singh, J. Appl. Phys., 1989, **65**: 1270.

[6] S. A. Knickerbocker and A. K. Kulkarni, J. Vac. Sci. Technol., 1995, **A13**(3): 1048.

[7] S. A. Agnihotry, K. K. Sari, T. K. Saxena *et al.*, J. Phys. D: Appl. Phys., 1985, **18**: 2087.

[8] K. L. Chopra, S. Major and D. K. Pandya, Thin Solid Films, 1983, **102**: 1.

[9] J. C. Manifacier, L. Szepessy, J. F. Bresse *et al.*, Mater. Res. Bull., 1979, **14**: 163.

[10] A. Azens, B. Stjerna, C. G. Granqvist *et al.*, Appl. Phys. Lett., 1994, **65**: 1998.

[11] W.-F. Wu, B.-S. Chiou and S.-T. Hsieh, Semicond. Sci. Technol., 1994, **9**: 1242.

[12] A. K. Kulkarni, K. H. Schulz, T.-S. Lim and M. Khan, Thin Solid Films, 1997, **308/309**: 1.

[13] Zhao Junqing, Ma Jin, Li Shuying, Ma Honglei, Chinese Journal of Semiconductors, 1998, **19**: 752 (in Chinese).

[14] P. Thilakan and J. Kumar, Vacuum, 1997, **48**: 463.

[15] C. D. Wagner, W. M. Riggs, L. E. Davis *et al.*, Handbook of X-ray Photoelectron Spectroscopy, Perkin-Elmer Corporation Physical Electronics Division, Printed in USA, 1979.

[16] N. Nadaud, N. Lequeux, M. Nanot *et al.*, J. Solid State Chem., 1998, **135**: 140.